

Article

Analysis of Lead Smelting Technology in the Early Bronze Age Based on Smelting Slag from the Central Plains of China

Shuoyang Li ¹, Yanxiang Li ¹, Rong Zhu ² and Hongyang Wang ^{2,*}

¹ Institute of Cultural Heritage and History of Science and Technology, University of Science and Technology Beijing, Beijing 100083, China

² School of Metallurgical and Ecological Engineering, University of Science and Technology Beijing, Beijing 100083, China

* Correspondence: b20180112@xs.ustb.edu.cn

Abstract: To explore the source of Pb in Bronze Age artefacts from the Central Plains (Zhongyuan) in China, we investigated non-ferrous minerals from the Qingyuan archaeological site in Yuanqu County near the Zhongtiao Mountains. Fragments of smelting slag from the Erlitou cultural layer were collected. The smelting slag was investigated by scanning electron microscopy (SEM), energy dispersive X-ray spectroscopy (EDS), X-ray photoelectron spectroscopy (XPS), X-ray diffraction (XRD), and lead isotope analysis. The SEM and EDS results confirmed that the slag contained Pb, Pb–As, and Cu–Pb–Sn inclusions and non-metal impurities such as low-Zn spinels. The XRD results signified that the bulk of the slag comprised Fe–Mn–Si phases. The chemical state of Pb was mainly Pb–O with some metallic Pb, as identified by XPS. The theoretical melting point was calculated using FactSage7.1 based on the composition and phase characterisation. The calculated temperature was 1100–1200 °C, which agreed well with the actual melting point of 1114–1354 °C. The slag composition and inclusion phases indicated that Pb–Zn–O ores with Mn and As were added during reduction smelting in Qingyuan. The raw materials of smelting included crude Pb with minor amounts of Cu, As, and Sn. Lead isotope analysis revealed that the lead materials produced in Qingyuan were likely transferred to Yanshi City in the Shang Dynasty. The findings of this study provide significant clues for exploring lead mineral production in the Central Plains during the Early Bronze Age.

Keywords: archaeometallurgy; Erlitou phase; lead smelting relic; lead isotopic ratio; Zhongtiao Mountains



Citation: Li, S.; Li, Y.; Zhu, R.; Wang, H. Analysis of Lead Smelting Technology in the Early Bronze Age Based on Smelting Slag from the Central Plains of China. *Metals* **2023**, *13*, 435. <https://doi.org/10.3390/met13020435>

Academic Editors: Petros E. Tsakiridis and Elena Gordo

Received: 8 January 2023

Revised: 6 February 2023

Accepted: 11 February 2023

Published: 20 February 2023



Copyright: © 2023 by the authors. Licensee MDPI, Basel, Switzerland. This article is an open access article distributed under the terms and conditions of the Creative Commons Attribution (CC BY) license (<https://creativecommons.org/licenses/by/4.0/>).

1. Introduction

The origins of metallurgy have been widely studied. Native copper has been processed in eastern Turkey since the end of the 9th millennium BC [1]. In Europe, evidence of copper smelting in the 5th millennium BC has been found in southeast Spain [2]. Between the 5th and 1st millennia BC, metalworking in Europe evolved from bronze to arsenic-doped copper [3] to tin bronze [4]. In China, significant progress has been made in understanding metalwork during the Early and Middle Bronze Age (2000–1000 BCE) in the last few decades. Issues such as the origins of Chinese metallurgy [5], compositional characteristics, and casting processes of bronze ceremonial vessels of the Xia and Shang [6] periods have always attracted the attention of scholars [7]. However, research based on metal artefacts only reflects the last steps of ancient metallurgical processes and does not explain the complete smelting process. We still do not know the technical details of early smelters' choices of ores and alloying methodologies [8]. Mining and smelting sites have been found in the Zhongtiao Mountains, which is considered to be the site of the earliest smelting in China [9]. After analysis of the above sites, scholars have identified red copper as the predominant smelting product of the Erlitou and Erligang cultures and made a preliminary identification of the industrial patterns of red copper smelting in the Zhongtiao Mountain area [10].

Tin bronze has several advantages, including corrosion resistance and a low melting point. It was widely used to produce weapons and ritual vessels before iron- and steel-making technology matured. However, tin bronze has poor castability. The walls of vessels formed from tin bronze are porous owing to the formation of dendritic grains during the early stages of solidification. In particular, heavy ritual vessels have high porosity because they were cooled gradually. This poor castability limited further application of tin bronze [11].

Adding lead to tin bronze to form a Cu–Sn–Pb ternary alloy significantly improves the ability of the molten alloy to flow and fill a mould, enabling the smoother casting of large, complex, and detailed objects. Therefore, lead had strategic economic importance in the Bronze Age and was an indispensable resource for casting large-scale bronze structures. Thus, only by simultaneously developing copper, lead, and tin smelting sites could the stable production of large bronze structures be ensured. However, an in-depth research is needed to ascertain whether lead and tin materials were produced in the Zhongtiao Mountain mining area during the Early Bronze Age.

In field investigations, a total of 33 bronze artefacts from the third to sixth phases of the Dongxiafeng site were unearthed [12]. Among these, five copper artefacts underwent a range of analyses, including wet chemical, qualitative spectrometric, and metallographic analyses. The results showed that two copper arrowheads from the fourth phase, a copper arrowhead from the fifth phase, and a copper utensil from the fifth phase were all lead–tin bronze or lead-bearing tin bronze [13]. Notably, the testing of an unearthed copper matte block with slag from the third phase suggested that the copper in this site was sourced from different sites to the tin- and lead-containing materials.

The analysis of six furnace slag and wall samples from the Upper Erligang Phase unearthed at the Yuanqu Shangcheng site at the southern foot of the Zhongtiao Mountains revealed that the copper alloy contained in these artefacts had three alloying elements, namely, tin, lead, and arsenic. Further, lead was added during copper melting [14]. In 2018, 293 copper-bearing lead ingots, weighing 3404 kg in total, belonging to the late stage of the fourth phase, were found in a storage pit in Liujiashuang Locus North, Yinxu. This provided further evidence that lead was used as a separate raw material for copper casting [15].

The aforementioned studies show that, in the Xia and Shang dynasties, the metallurgical technologies used in the Zhongtiao Mountains area enabled the production of tin bronze, lead bronze, and lead–tin bronze. The alloying method used involved the addition of metallic tin and lead (possibly arsenic-bearing) to red copper. Further, research on copper-casting sites in settlements in the regional centres and capital of the kingdom showed that there were likely separate sources of lead and tin. However, to date, there has been almost no investigation of lead–tin smelting sites in the Zhongtiao Mountain area from the Xia, Shang, and Zhou dynasties. Pre-Qin archaeological sites known to contain artefacts of lead-melting processes include Yangxin County, Huangshi [16]; the Shuzhuangtai site in the ancient city of Zhenghan in Xinzheng, Henan [17]; and the Shifotang site in the ancient city of Qi in Linzi, Shandong [18].

Following up on previous mining and metallurgical investigations, the investigation of the Erlitou cultural layer of the Qingyuan site in Yuanqu County resulted in the discovery of lead-bearing smelting slag. After sampling, the basic composition of the slag was determined using multiple experimental methods, including scanning electron microscopy–energy dispersive X-ray spectroscopy (SEM-EDS), X-ray photoelectron spectroscopy (XPS), and X-ray diffraction (XRD). FactSage7.1 (Thermfact/CRCT, Montreal, Quebec, Canada and GTT-Technologies, Aachen, Germany) was used to obtain a phase diagram based on the geological characteristics of the lead ore resources in the Zhongtiao Mountain area and predict the possible smelting temperatures and technologies used at the time of production. Subsequently, the actual melting temperature of the slag was determined and found to be consistent with the predicted value. In addition, the lead isotope characteristics of the slag obtained from the Qingyuan site were similar to those of bronze artefacts unearthed

at the Shangcheng site in Yanshi. In summary, the discovery of this lead smelting site in Qingyuan suggests that a relatively developed lead smelting technology was used as early as the Xia and Shang periods in the Zhongtiao Mountain area. This preliminary study fills a gap in research concerning lead smelting sites during the Xia and Shang dynasties in the core area of the Central Plains. However, the current findings are based on a small-scale study, and the investigation of further sites is required.

2. Materials and Methods

2.1. Site Location, Field Investigation, and Dating

The archaeological site is located in Yuanqu County, on a high plateau (altitude of 500–522 m) northeast of the Zhongtiao Mountains, to the west of Yangjiahe Natural Village in Qingyuan Administration Village. It is surrounded by water on the east, west, and south, adjacent to the Qingyuan River (a seasonal stream) on the east and surrounded by the Shiba River (a branch of the Boqing River) on the west and south. The site is 5 km from the Zhongtiao Mountains and has an area of 40,000 m². The location and topography of the site region are shown in Figure 1, and a photograph of the surrounding area and archaeological layers where relics were identified is shown in Figure 2.

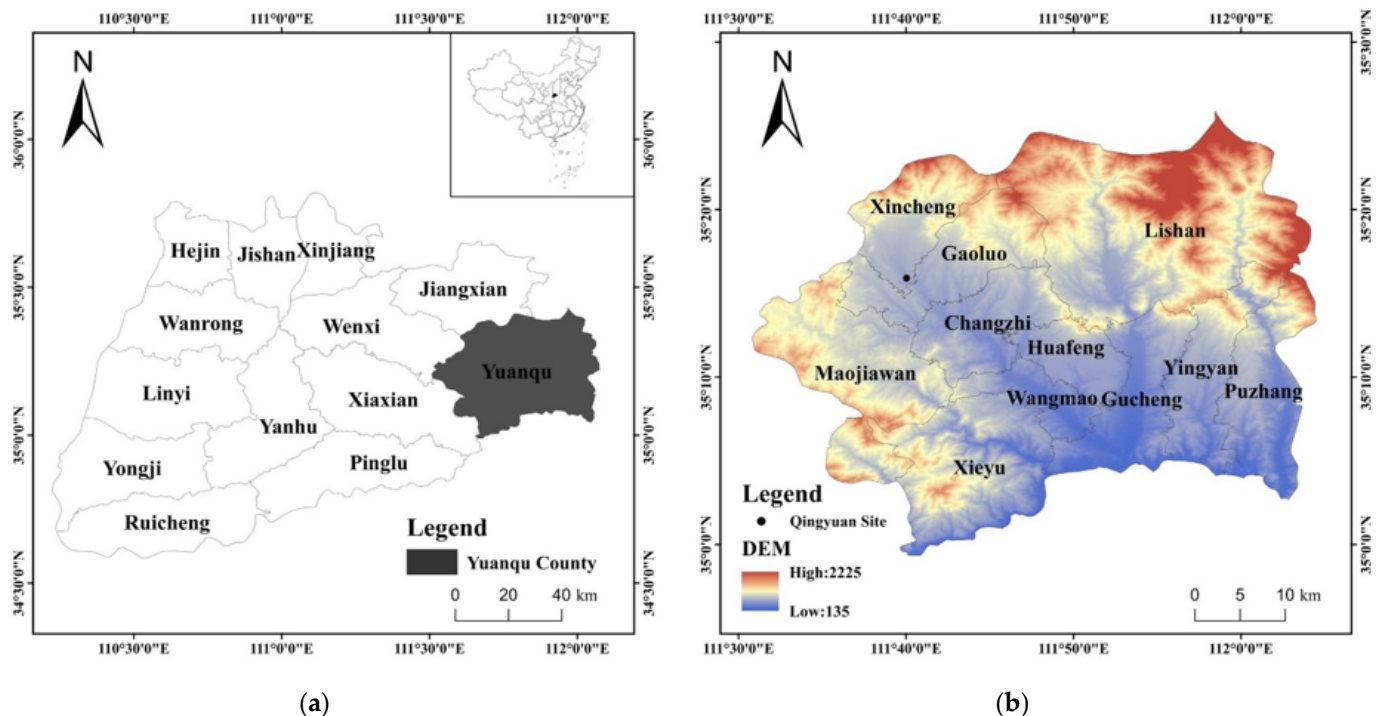


Figure 1. (a) Location and (b) topographic map of Yuanqu County. The Qingyuan site is marked with a black spot in (b).

In 1982, members of the Archaeology Department of the National Museum of Chinese History and the Yuanqu County Museum jointly conducted an investigation in which they collected artefacts such as grey and painted pottery pieces at this site. Further investigations were conducted at this site between 2001 and 2003 by members of the Archaeology Department of the National Museum of China. After these investigations, the site was deemed to include cultural artefacts from four cultures in different periods: the late Yangshao culture, the Miaodigou culture of Phase II, the Longshan culture, and the Erlitou culture [19].

In this study, ground and cross-sectional observations revealed that the cultural relics were mainly distributed in the terraced fields on the north slope of Zhongtiao Mountain, even though some features, such as ash pits, were exposed on some sections of the terraced fields.

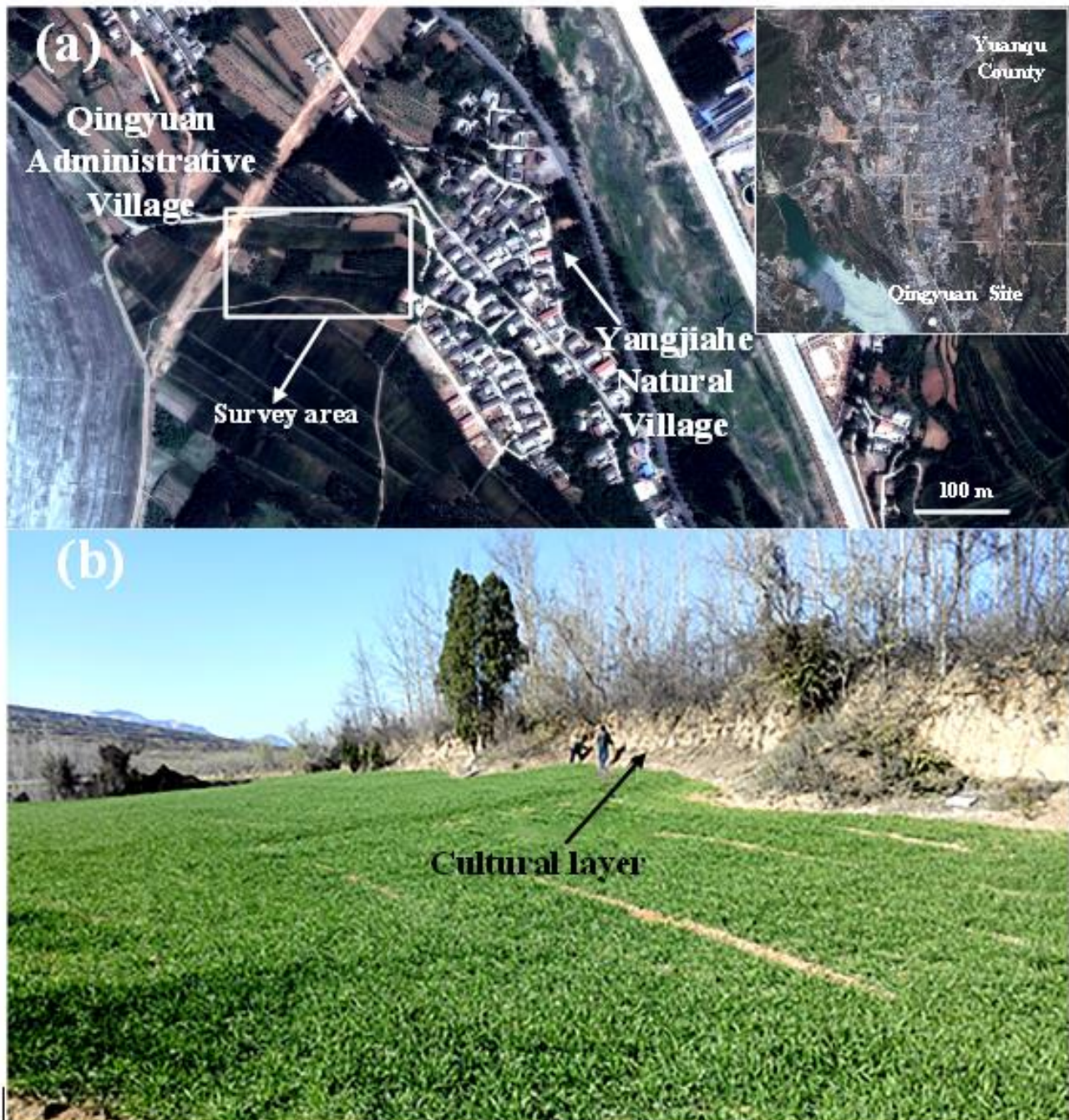


Figure 2. (a) Satellite map of the smelting district Qingyuan site. (b) Cultural layers containing relics from different cultures at the Qingyuan site.

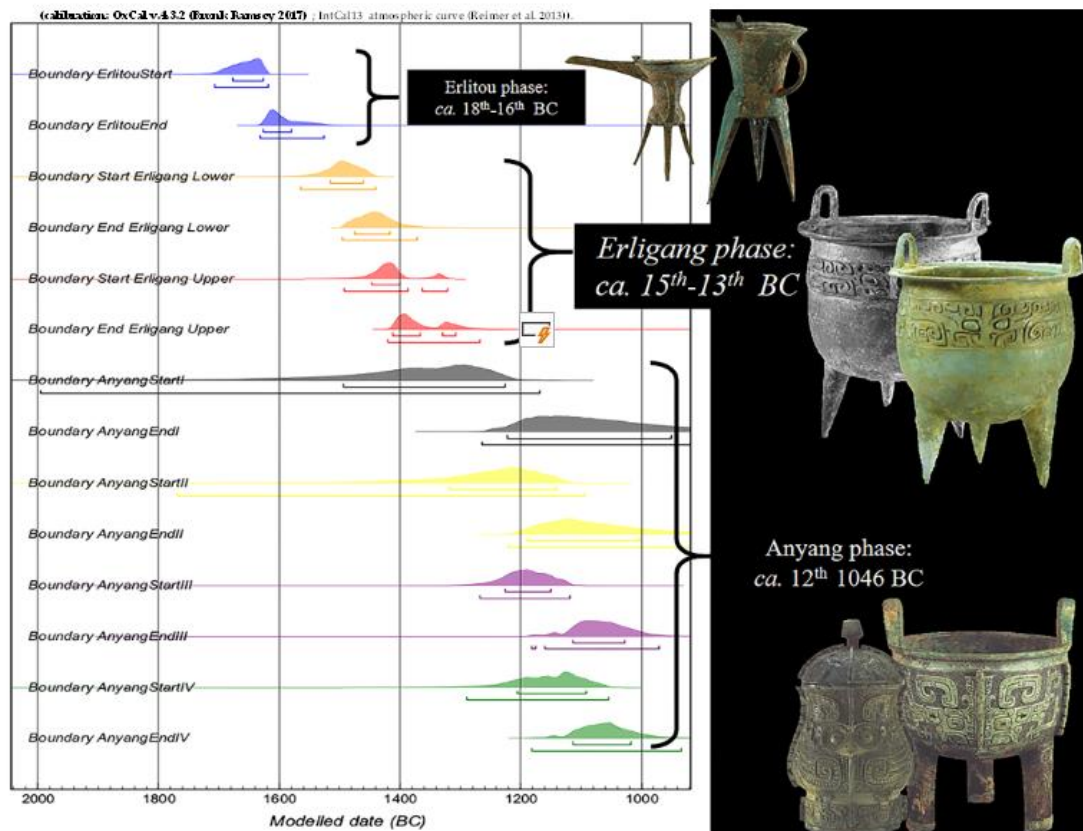


Figure 3. Chronological framework of the early Bronze Age in the Central Plains, China [20].

The chronological framework of the Early Bronze Age in central China is shown in Figure 3.

Pottery pieces from the Erlitou culture period were found in the ash pit at the Qingyuan site (Figure 4). Therefore, all samples were analysed on-site using a portable X-ray fluorescence (pXRF) spectrometer to discriminate ancient ‘kiln sweat’ (the glassy slag that forms in pottery kilns) [21] from smelting slag because of their similar appearance.

2.2. Collected Slag Samples

Eleven slag artefacts were collected from the Qingyuan site. The slag artefacts were non-magnetic and had a black glassy appearance (Figure 5) with hard and shiny surfaces and some surface porosity. Based on appearance, these slag artefacts were judged to be produced during high-temperature melting.



Figure 4. Pottery pieces from the Erlitou culture period collected from the ash pit. Fragment 1: a sand-filled piece of brown pottery, possibly the edge of a piece with a round lip. Fragments 2–4: small fragments of muddy brown pottery. Rope-like patterns and other indistinguishable shapes are present on the surface.



Figure 5. Appearance of slag samples from the Qingyuan site.

2.3. Compositional and Phase Identification

SEM (TESCAN, Czech Republic) was used to observe the sample morphology, and EDS (Bruker, German) was used to quantitatively analyse the sample composition. Backscattered electron imaging was used for phase identification with an accelerating voltage of 20 kV, a working distance of 15 mm, and an acquisition time of 60 s. EDS point analyses were conducted on areas with minimal porosity. At least three areas were analysed for each sample, and the results were averaged. Elements such as C and O were excluded from the results, and the contents of the remaining elements were normalised.

To characterise Pb in the slag samples, XPS and XRD were used for analysing the chemical states and phases of the samples, respectively. Combining the results enabled qualitative analysis of the phase composition. XPS analysis was conducted using a Thermo ESCALAB250xi spectrometer (Thermo Fisher Scientific, Waltham, MA, USA). The analysis area, pass energy, and step size were $200 \mu\text{m}^2$, 30.0 eV, and 0.1 eV, respectively. The number of points for energy analysis was 401. XRD analysis was conducted using an Ultima IV diffractometer (Rigaku, Japan) at a voltage and current of 40 kV and 40 mA, respectively. The samples were scanned in the 2θ range of 10° – 90° at a rate of 10°min^{-1} . Before analysis, each sample was pulverised, placed in the sample container, compacted and flattened with a glass slide, and then placed on the sample stage.

The melting points were measured using an automatic slag melting point and melting rate tester (RDS-04, Northeastern University, China). The temperature at which the sample shrinkage reached 75% (i.e., when 75% of the sample had melted) was taken as the melting point.

Because of large variations in the sample quality and size, for the XPS and XRD analyses, all eleven slag samples were pulverised to a powder using a pestle and mortar, sieved to 200-mesh, and mixed together. The mixed powder was then separated into two groups (A and B) to ensure the accuracy of the test results. Grinding was performed in a natural agate mortar with strong corrosion resistance and high hardness to prevent sample contamination during pulverisation.

2.4. Characterisation of the Direction of Material Flow through Pb Isotope Analysis

The Pb isotope ratio is characteristic of a given mining area [22]. Crucially, the Pb isotopes do not undergo fractionation during smelting; thus, their ratio remains unchanged in the final product [23]. Consequently, the Pb isotope ratios of bronze relics and slag artefacts can be compared for an approximation of the circulation and spread of raw materials during the period in which the artefacts were produced, and valuable information for archaeo-metallurgical research can be obtained [24].

Pb isotope analysis was conducted using a multi-collector inductively coupled plasma mass spectrometer (MC-ICP-MS, Neptune Plus, Thermo Fisher Scientific, USA) following the Chinese National Standard GB/T 31231-2014 ('Determination of zinc and lead isotopic ratios in aqueous solution. Multiple-collectors inductively coupled plasma mass spectrometry'). Briefly, the Pb-bearing sample was fully dissolved and dropped in a rhenium or tantalum trough with a width of 1–2 mm (coated with an emitting agent to improve the emission efficiency). Then, the solution was dried, and the trough was placed in the sample chamber, which was evacuated to a high vacuum. Subsequently, the current was applied to the trough with heating to 1200 °C to ionise the sample. In the analysis chamber, the Pb ions were accelerated by the electric field and selectively separated by the magnetic field. On impacting the sensing plate of the ion receiving system, the generated current was amplified to yield the following isotope ratios: $^{206}\text{Pb}/^{204}\text{Pb}$, $^{207}\text{Pb}/^{204}\text{Pb}$, and $^{208}\text{Pb}/^{204}\text{Pb}$ [25].

2.5. Analysis of Metallurgical Processes

FactSage7.1 was used to obtain the phase diagrams for slag melting during the smelting process from the chemical compositions and phase profiles of the slag samples. The phase diagrams were then used to assess possible smelting technologies and sources of the raw and furnace materials based on the local geological and mineralogical characteristics.

3. Results and Discussion

3.1. Sample Composition and Morphology

The chemical compositions of the slag samples are listed in Table 1. The main components were SiO_2 , MnO , and FeO , followed by Al_2O_3 , MgO , and CaO , with small amounts of Na_2O and K_2O .

Table 1. Chemical composition of 11 Qingyuan slag samples.

Sample	Chemical Composition (wt%)									
	Na_2O	MgO	Al_2O_3	SiO_2	K_2O	CaO	MnO	FeO	ZnO	Pb
QY001	0.53	1.53	5.57	42.69	0.15	3.64	11.27	34.35	0.17	-
QY002	0.34	1.39	4.83	42.82	0.18	4.11	11.44	34.80	0.10	-
QY003	0.21	1.69	4.90	41.72	0.21	4.22	11.38	35.66	0.00	-
QY004	0.70	1.48	5.11	41.73	0.18	4.39	11.15	35.12	0.13	-
QY005	0.68	1.49	4.88	41.08	0.28	4.31	11.41	35.74	0.13	-
QY006	1.10	1.13	8.34	29.97	0.47	7.84	10.88	35.09	5.19	1.00
QY007	1.31	1.16	9.28	33.32	0.47	7.92	10.18	31.11	5.25	2.53
QY008	1.10	0.77	8.27	30.18	0.53	7.71	11.55	35.21	4.67	0.64
QY009	0.91	0.98	8.45	30.87	0.55	8.33	10.88	33.58	5.44	0.68
QY010	1.18	0.97	9.16	32.32	0.46	7.39	11.06	33.12	4.35	0.56
QY011	0.33	2.04	7.58	22.18	2.09	15.07	21.05	25.94	3.72	0.99

The samples were divided into three types based on the morphology and composition of the inclusions. In the first type, metallic Pb particles were detected by optical microscopy; in the second type, no Pb-rich phases were found; and in the third type, the Pb-bearing particles were too small to be detected by optical microscopy, but EDS analysis revealed Pb-rich particles that contained Cu and Sn precipitates.

3.1.1. Slag Samples with Metallic Pb Inclusions

Representative micrographs of the slag samples with metallic Pb inclusions are shown in Figure 6. Sample QY001 contained several types of inclusions (Figure 6c) that were identified as metallic Pb, fayalite (Fe_2SiO_4), and hercynite (an iron spinel, FeAl_2O_4).

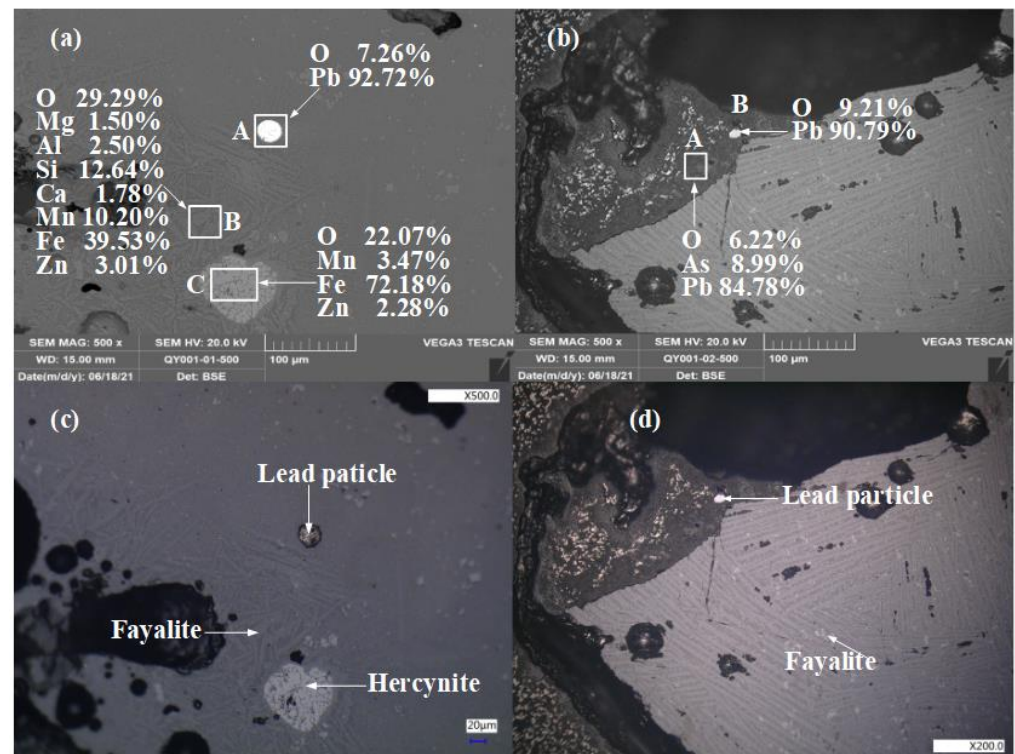


Figure 6. (a,b) SEM backscattered electron images and (c,d) optical micrographs of samples (a,c) QY001 and (b,d) QY002 at the same scale. The same region of each sample is shown in the SEM and optical images.

In addition, EDS analysis (Figure 6a) showed that Mn, Fe, and Zn were distributed in the fayalite and spinel phases. Sample QY002 also contained metallic Pb particles and fayalite inclusions (Figure 6b). In addition, PbO particles were observed. EDS analysis of this sample (Figure 6d) showed that the metallic Pb particle contained a smaller Pb–As–O phase (marked 'A' in Figure 6d).

3.1.2. Slag Samples without Pb-Rich Phases

Representative micrographs of the slag samples without Pb-rich phases are shown in Figure 7. Sample QY008 contained lath-shaped fayalite and hercynite phases (Figure 7c). EDS analysis also indicated the presence of V and Cr in the hercynite phase and Mn and Zn in the hercynite and fayalite phases (Figure 7a).

The content of Mn and Zn in the hercynite phase was higher than that in the fayalite phase. The inclusions in sample QY009 (Figure 7b) and their components were similar to those in sample QY008.

The lath-shaped fayalite particles were distributed throughout the sample matrix, and V- and Cr-bearing hercynite particles were included in the fayalite phase (Figure 7d).

3.1.3. Slag Samples with Small Pb-Bearing Particles and Cu and Sn Phases

Representative micrographs of slag samples with small Pb-bearing particles and Cu and Sn phases are shown in Figure 8. As-containing Pb-rich particles were detected in sample QY010. The main elements in the slag matrix were Mn, Fe, Zn, and S.

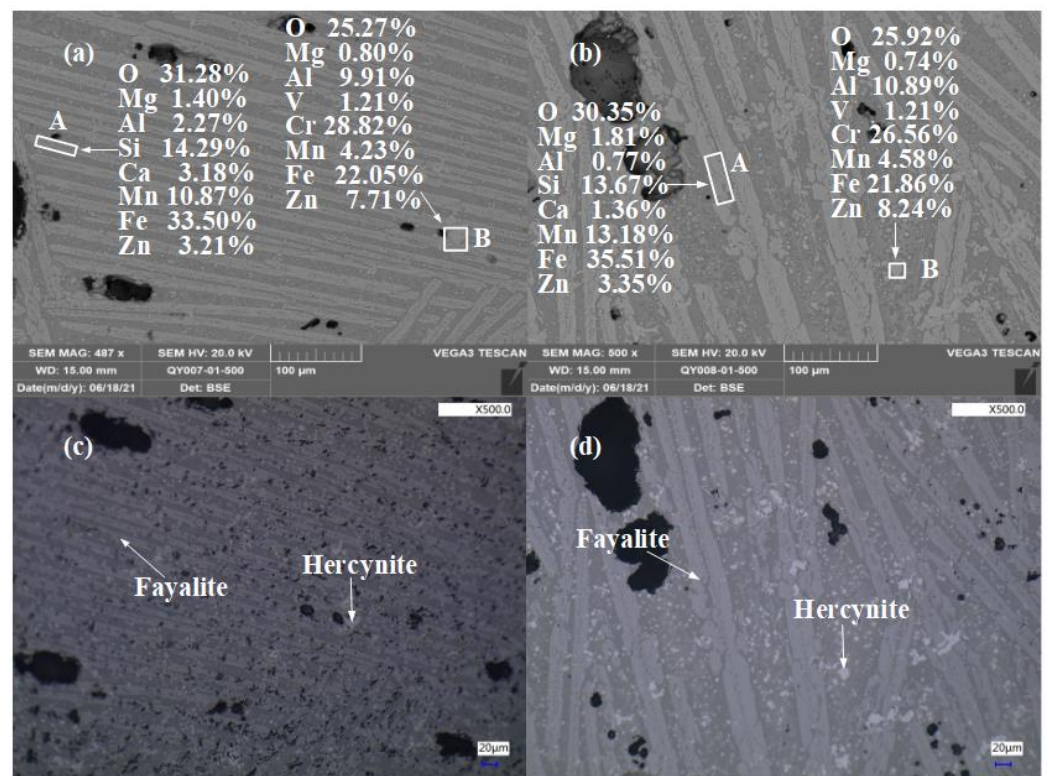


Figure 7. (a,b) SEM backscattered electron images and (c,d) optical micrographs of samples (a,c) QY008 and (b,d) QY009 at the same scale. The same region of each sample is shown in the SEM and optical images.

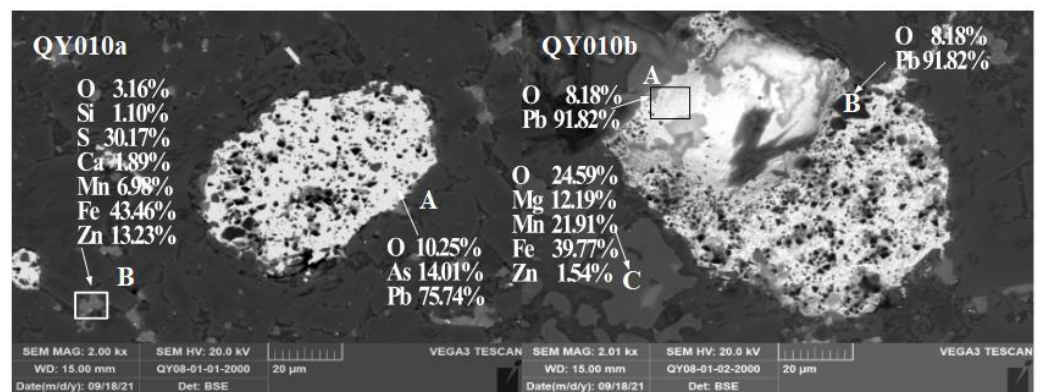


Figure 8. SEM backscattered electron images of sample QY010 with Pb-bearing particles.

EDS elemental mapping of sample QY010 (Figure 9) showed that Cu and Sn were included in the Pb-based particles in this sample, whereas Mn and Fe were distributed in the slag matrix as fayalite.

3.2. Main Phases and Chemical States of Pb in the Samples

Figure 10 shows the XPS profile of the Pb region of a mixed powder of samples QY001–QY011. The slag samples were pulverised and mixed before the XPS analysis to ensure the accuracy of the test results, considering the large variations in sample quality and size. The main chemical forms of Pb were Pb–O and metallic Pb, with Pb–O accounting for a larger proportion. This finding agrees with the microscopy and SEM analysis results.

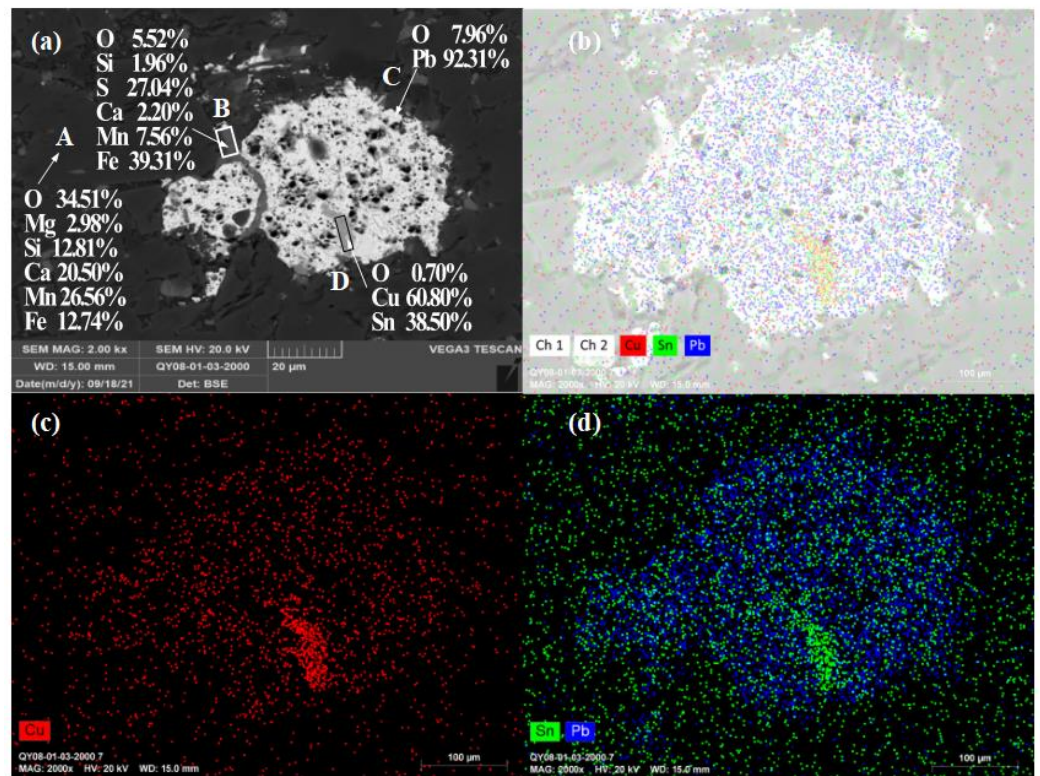


Figure 9. (a) SEM backscattered electron image of Pb-bearing particle in QY010 and (b–d) EDS elemental mapping images of the region in (a). (b) Cu + Sn + Pb, (c) Cu, and (d) Sn + Pb.

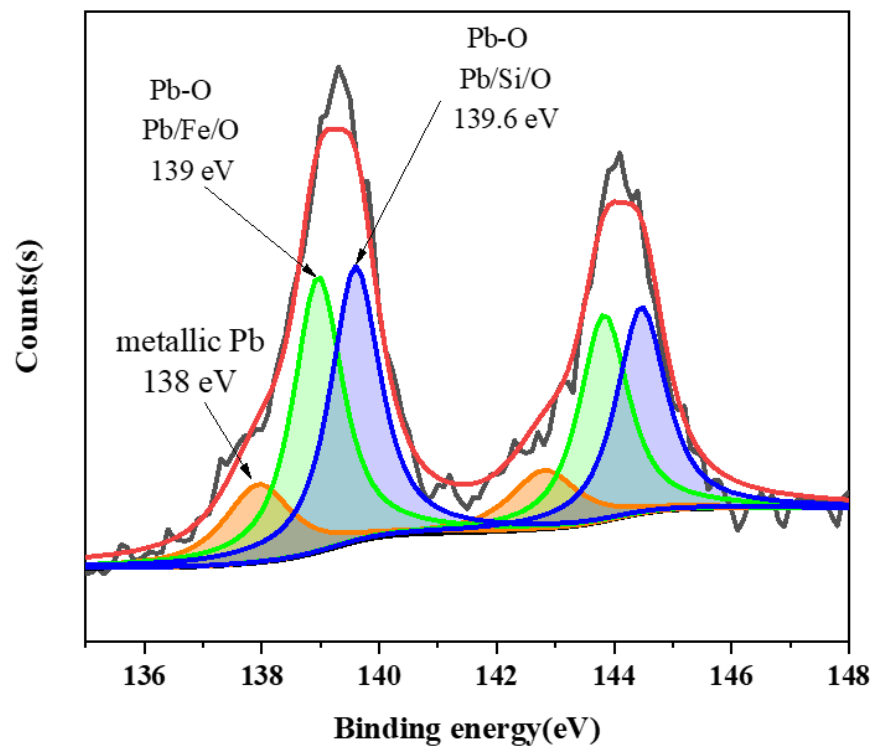


Figure 10. X-ray photoelectron spectrum of a mixed powder of samples QY001–QY011.

XRD patterns of the mixed powders of samples QY001–QY011 are shown in Figure 11. The dominant phases were fayalite and other silicates. From the elemental compositions and XRD patterns, the possible phases were determined (Table 2).

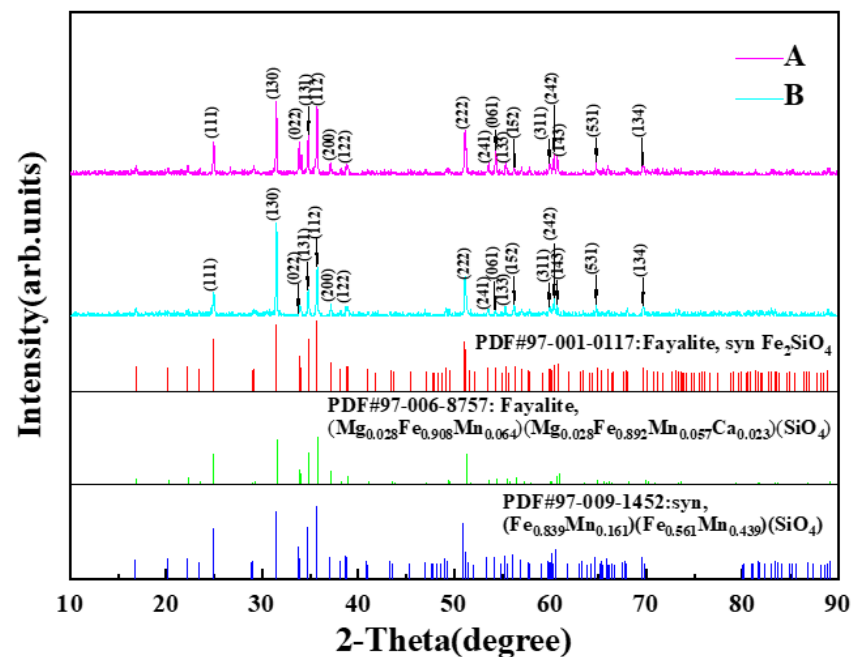


Figure 11. XRD patterns of mixed powders of samples QY001–QY011 (A and B are two equivalent mixtures of samples QY001–QY011) and reference patterns of various potential silicate phases, including fayalite.

Table 2. Proposed Fe-, Mn-, Mg-, and Ca-containing phases in the slag samples.

Element	Proposed Phases
Fe	Fe_2SiO_4 , $(\text{Fe},\text{Mn})_2\text{SiO}_4$, $(\text{Mg}_{0.028}\text{Fe}_{0.908}\text{Mn}_{0.064})(\text{Mg}_{0.028}\text{Fe}_{0.892}\text{Mn}_{0.057}\text{Ca}_{0.023})(\text{SiO}_4)$
Mn	$(\text{Fe},\text{Mn})_2\text{SiO}_4$, $(\text{Mg}_{0.028}\text{Fe}_{0.908}\text{Mn}_{0.064})(\text{Mg}_{0.028}\text{Fe}_{0.892}\text{Mn}_{0.057}\text{Ca}_{0.023})(\text{SiO}_4)$
Mg	$(\text{Mg}_{0.028}\text{Fe}_{0.908}\text{Mn}_{0.064})(\text{Mg}_{0.028}\text{Fe}_{0.892}\text{Mn}_{0.057}\text{Ca}_{0.023})(\text{SiO}_4)$
Ca	$(\text{Mg}_{0.028}\text{Fe}_{0.908}\text{Mn}_{0.064})(\text{Mg}_{0.028}\text{Fe}_{0.892}\text{Mn}_{0.057}\text{Ca}_{0.023})(\text{SiO}_4)$

The analysed slag samples had the following characteristics. First, the contents of Fe and Mn (as FeO and MnO, respectively) were relatively high, with FeO and MnO accounting for approximately 36 and 12 wt% of the samples, respectively. Fe and Mn were enriched in the fayalite and silicate phases commonly found in smelting slag. Second, the samples also contained Ca (as CaO), with CaO contents up to 15.07 wt%. Most samples had a CaO content of 3.64–8.33 wt%. Third, the samples had either high or low Zn contents (calculated as ZnO). Finally, Pb particles with round or quasi-circular irregular shapes were detected in the samples with higher Zn contents (calculated as ZnO). A small amount of As was found in these Pb-based particles, and Cu and Sn were found in the Pb-rich particles in sample QY011.

3.3. Physicochemical Characteristics of the Samples

For the production of slag during smelting, the melting point of the slag must be controlled. This also improves the fuel efficiency of the smelting process. The equilibrium ternary phase diagram of FeO–SiO₂–MnO was obtained using FactSage7.1. As shown in Figure 11, the slag composition with the lowest melting point is 12–25 wt% MnO and 13–24 wt% SiO₂. However, the investigated slag artefacts had MnO and SiO₂ contents of 10.18–21.05 and 30.18–42.82 wt%, respectively, as indicated by the black spots in Figure 12. The measured data were normalised and then projected onto the phase diagram. From the projected data, we determined that the melting point of the slag was as high as 1400–1600 °C. Such a high smelting temperature was not achievable with the technological abilities of the Erlitou culture; thus, it is not compatible with the archaeological cultural background.

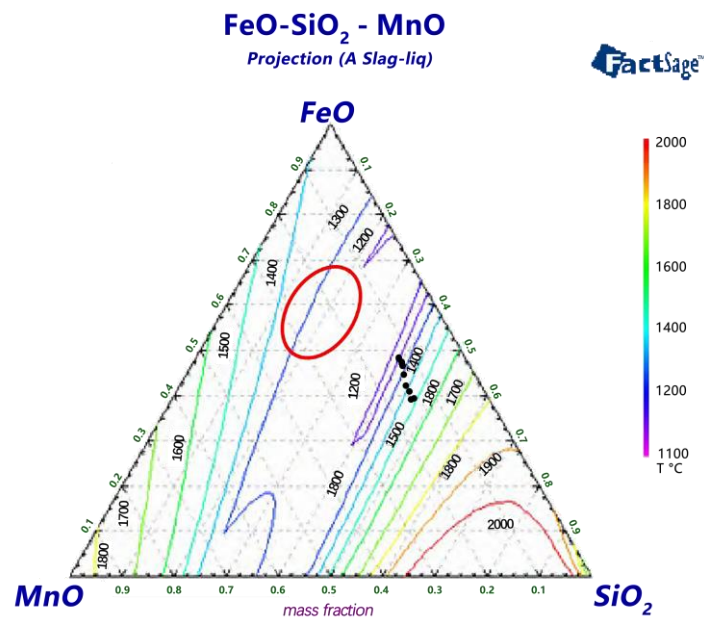


Figure 12. Equilibrium ternary phase diagram of FeO–SiO₂–MnO [26].

During smelting, the CaO in the ore only participates in fluxing after fully participating in slagging. Therefore, a multi-component Al₂O₃–SiO₂–CaO–MnO–FeO–MgO model was determined based on the measured data. Figure 13 shows the final results.

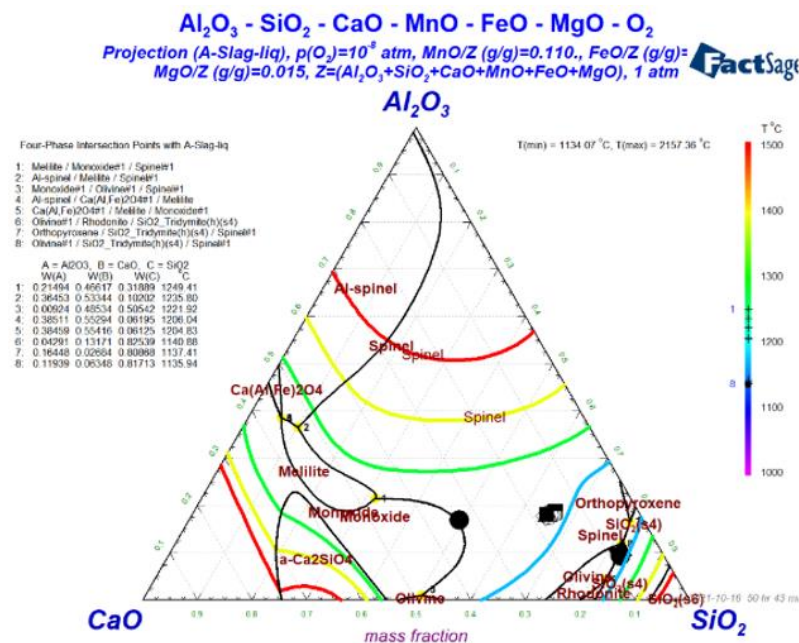


Figure 13. Iso-liquidus diagram based on the actual composition of the slag. Al₂O₃ – SiO₂ – CaO – MnO (11%) – FeO (34%) – MgO (1.5%) – O₂, P(O₂) = 10⁻⁸ atm.

The calculation results based on the multi-component model indicate that the melting point of the slag was 1100–1300 °C. To confirm this, 4 of the 11 samples were used for melting point analysis using an RDS-04 automatic slag melting point and melting rate tester. The results are plotted in Figure 14.

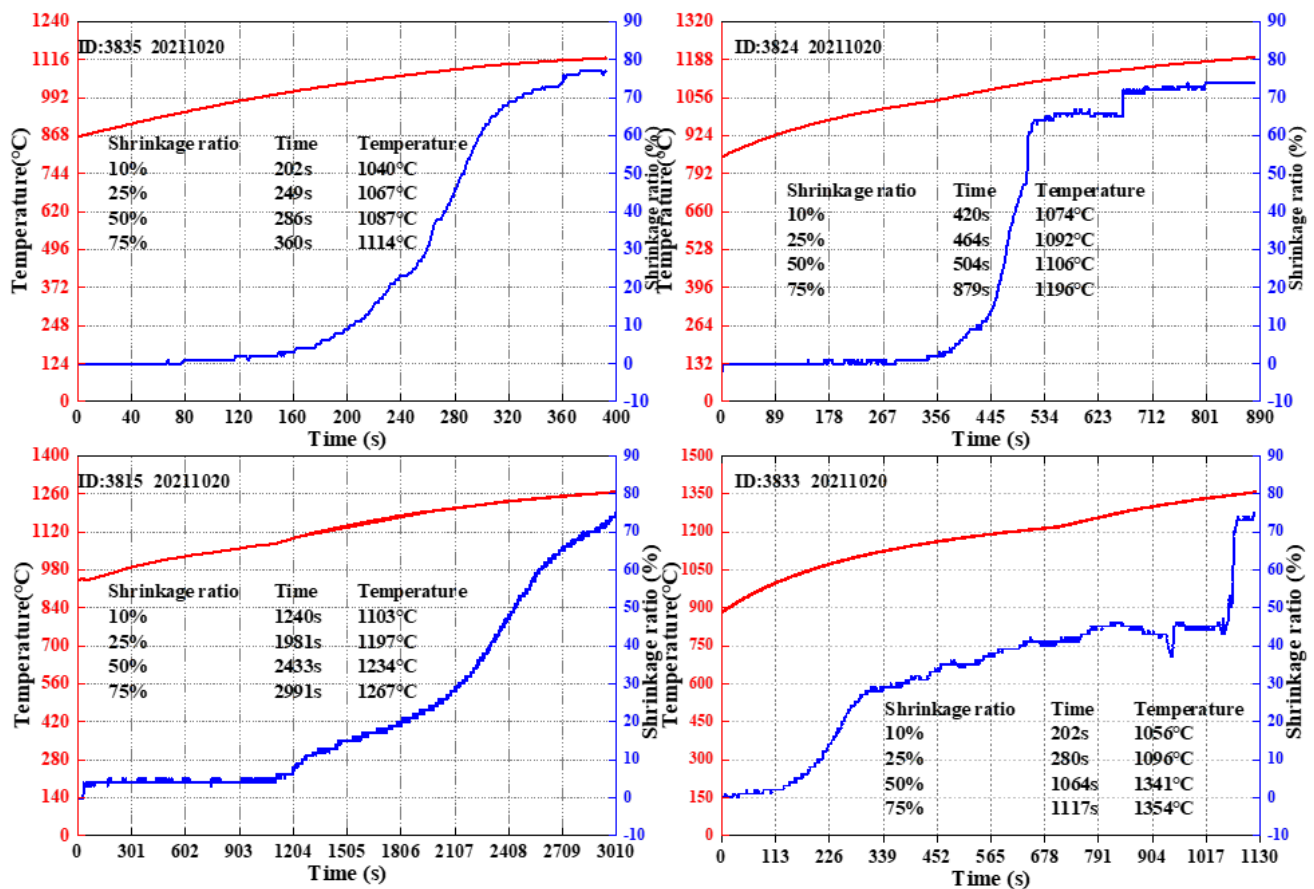


Figure 14. Results of melting rate tests for four slag samples.

The slag was considered to be molten when the shrinkage rate reached 75%; therefore, the corresponding temperature was recorded as the melting point. The melting points of the four samples were 1114, 1196, 1267, and 1354 °C, which are highly consistent with the simulation results. Moreover, they fall within the regions of smelting (900–1200 °C) and hearth (1200–1300 °C) zones that are reached during the reduction and refining of Pb compounds to produce Pb in modern blast furnaces.

3.4. Characterisation of Pb Isotopes

The Pb isotopes were characterised by plotting the $^{207}\text{Pb}/^{204}\text{Pb}$ and $^{208}\text{Pb}/^{204}\text{Pb}$ ratios of the slag samples against the $^{206}\text{Pb}/^{204}\text{Pb}$ ratios (Figure 15a,b, respectively).

The results of lead ore samples obtained from the Shenxianling and Laojunmiao sites in the lead belt to the south of Zhongtiao Mountain were also plotted. Ellipses showing the 95% confidence intervals were drawn. There was little-to-no overlap of the ellipses, indicating that the Pb isotope ratios of these samples differ significantly; consequently, the Pb is unlikely to have been sourced from these sites.

Figure 16 shows the Pb isotope characteristics of the slag samples along with those of bronze artefacts obtained from the Yanshi Shangcheng site (Early Shang dynasty) near Zhongtiao Mountain.

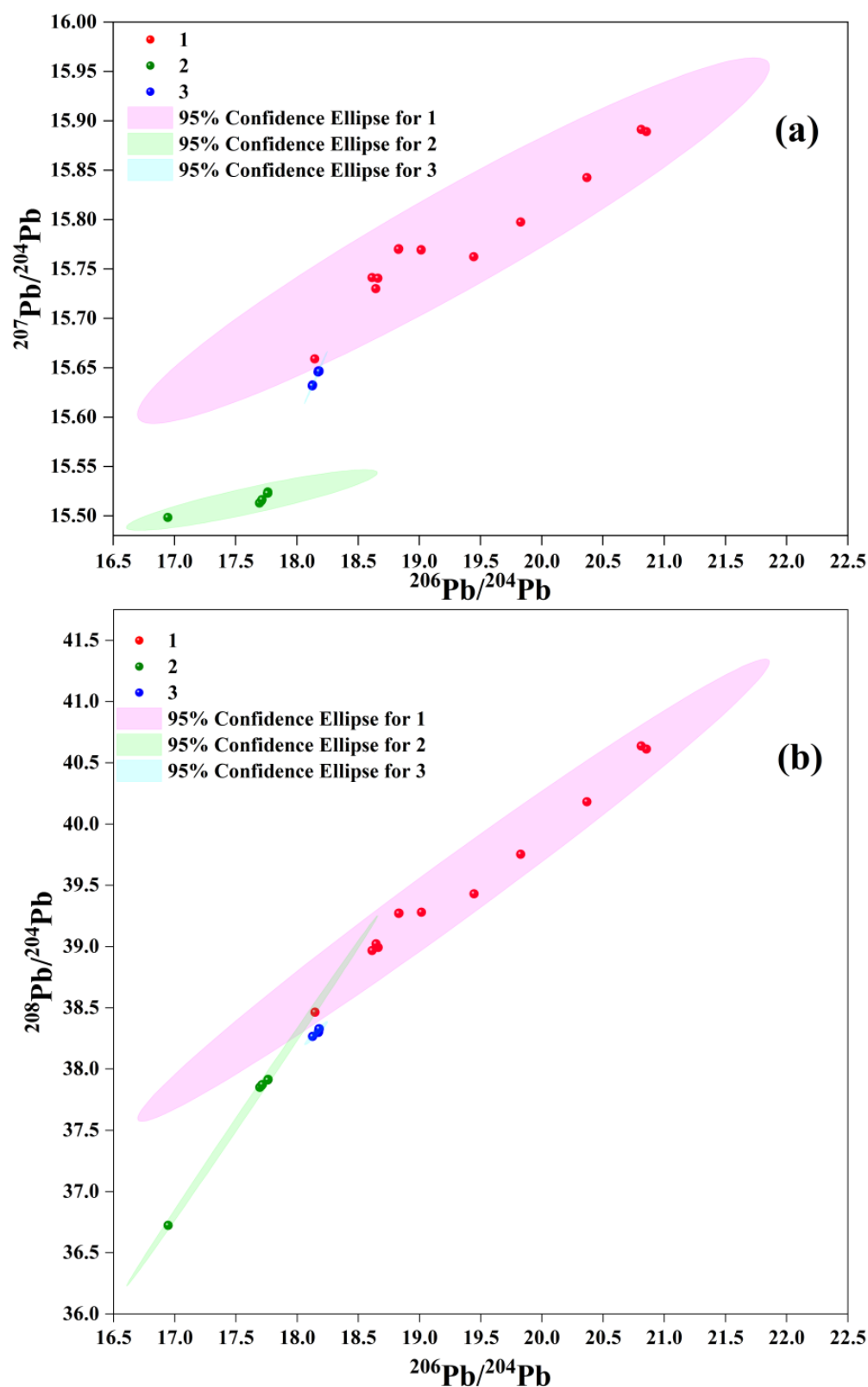


Figure 15. Comparison of Pb isotopes in different samples. (a) $^{207}\text{Pb}/^{204}\text{Pb}$ and $^{206}\text{Pb}/^{204}\text{Pb}$ ratios of the slag samples; (b) $^{208}\text{Pb}/^{204}\text{Pb}$ and $^{206}\text{Pb}/^{204}\text{Pb}$ ratios of the slag samples; 1: Slag from the Qingyuan site; 2: lead ore deposits from the Shenxianling site; and 3: lead ore deposits from the Laojunmiao site.

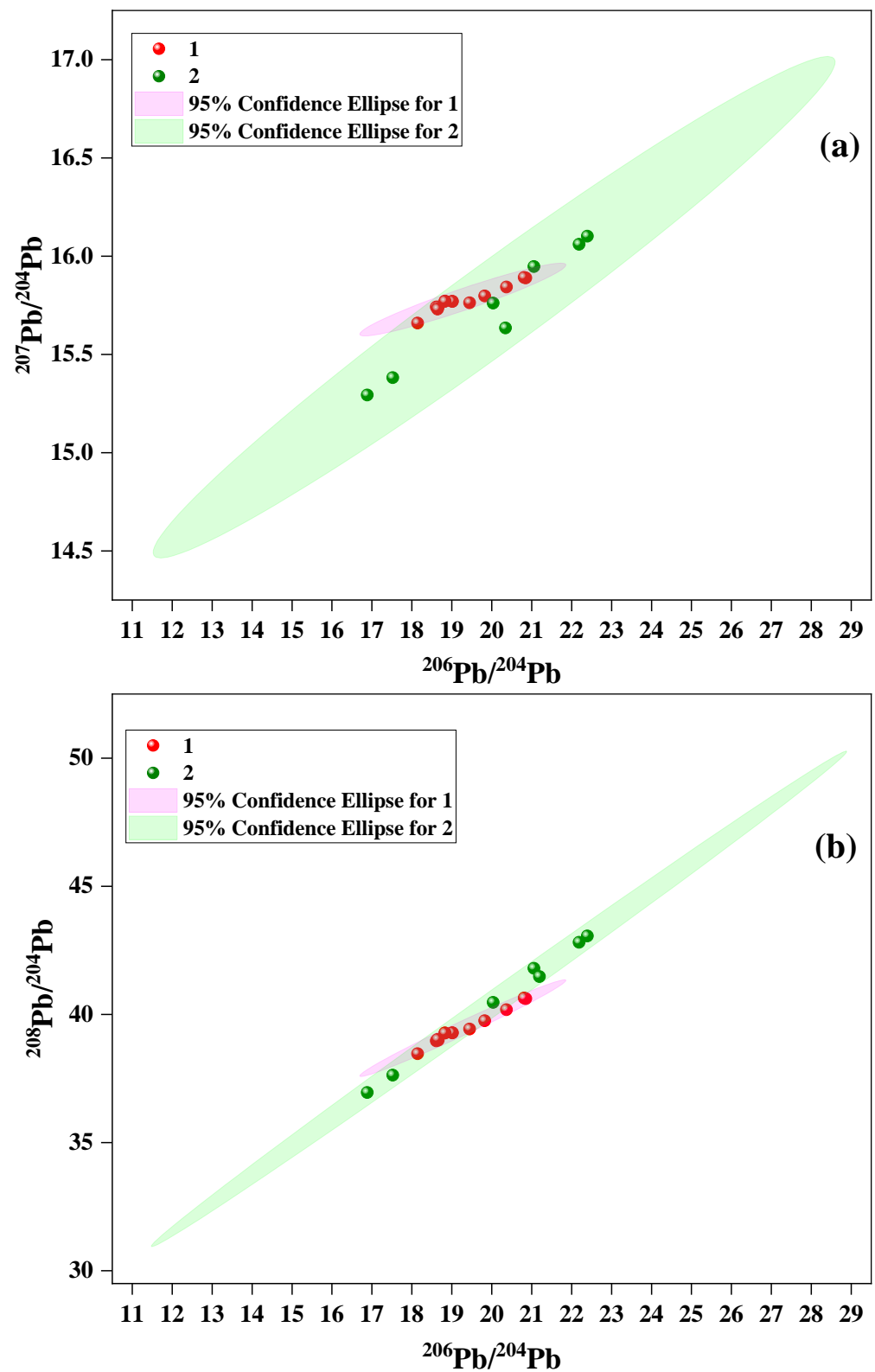


Figure 16. Comparison of Pb isotopes in different samples. (a) $^{207}\text{Pb}/^{204}\text{Pb}$ and $^{206}\text{Pb}/^{204}\text{Pb}$ ratios of the slag samples; (b) $^{208}\text{Pb}/^{204}\text{Pb}$ and $^{206}\text{Pb}/^{204}\text{Pb}$ ratios of the slag samples; 1: Slag from the Qingyuan site and 2: Bronze artefacts from the Yanshi Shangcheng site [27] (Early Shang dynasty) near Zhongtiao Mountain.

The 95% confidence intervals of the Pb isotope ratios overlapped significantly (within the 95% confidence interval), suggesting that the Pb in both sample types could have been sourced from the same site.

3.5. Analysis of the Ore Origin and Smelting Technology

Mineral resources and natural conditions significantly affect the layout of mining and metallurgical operations, including the reserves, grades, burial conditions, and geographical location of mineral resources. The piedmont-inclined plain where the site is located is covered with deep loess, providing rich crop nutrients. The plain has a relatively high altitude, which prevents flooding, and is close to a river, which makes it suitable for farming and human settlement.

Lead ore is composed of Pb-bearing minerals, symbiotic minerals, and gangue and can be classified into sulphide and oxide ores. The area in the south-central Zhongtiao Mountains where lead ore is predominantly distributed is in a copper-polymetallic mineralised zone [28]. Notably, the Hu-Bi-type Cu deposits include mineralised Pb and Zn in some parts [29]. Further, the concentration of Mn is higher than the background values of crustal elements [30]. Geological studies have shown that Pb-bearing minerals such as galena, stannite, lillianite, and kocharite are distributed in the Hu-Bi-type Cu deposit area of the Zhongtiao Mountains [31]. These ore sites are within 20–40 km from the current site, and ore could quickly travel between them via mountain canyons or rivers, effectively reducing transport costs. The Lead ore sites near the Qingyuan site are shown in Figure 17.

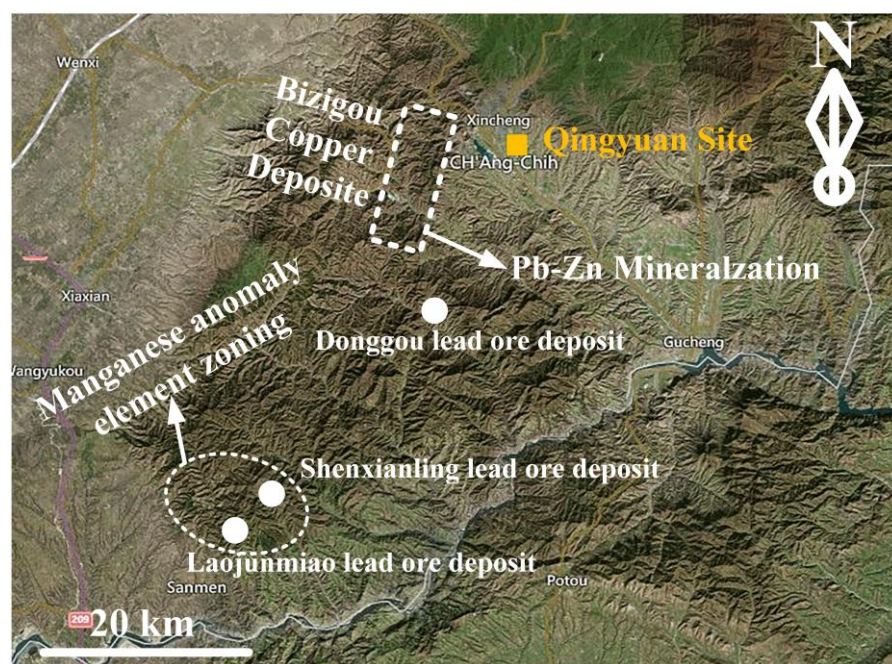


Figure 17. Lead ore sites around the Qingyuan site.

Located within 40 km from the site is the Liujiacha–Zuizishan mining area in Pinglu County on the southwestern margin of the Zhongtiao Mountains, which represents a polymetallic ore belt where Pb, Zn, and Sn anomalies have been detected [32]. The above-mentioned areas were the key areas investigated when searching for ancient lead ore in the Zhongtiao Mountains. However, the deposits discovered thus far are relatively few and small-scale; nevertheless, they include Pb–Zn–Ag deposits near the Nanbai Mountain in Laojunmiao [33]. In addition, petrochemical surveys have been conducted in the Liumuzhuo, Nanbai Mountain, and Wazhagou areas, and an Mn anomaly with a value of 13,830 (unit 10^{-6}) has been found [34]. This area will be the focus of further investigations on Pb mining and smelting relic sites. Based on the Pb isotope data, we speculated that

some of the Pb materials used at the Yanshi Shangcheng site originated from the same mining area as that of the Qingyuan site or that the minerals at the two sites were from two different sources within the polymetallic ore belt in the Zhongtiao Mountains.

Galena (PbS), a primary mineral, is the most widely distributed lead ore in this area and is commonly symbiotic with sphalerite (ZnS), pyrite (FeS₂), and chalcopyrite (CuFeS₂) [35]. The gangue minerals associated with galena are limestone (CaCO₃), quartz (SiO₂), and barite (BaSO₄) [36]. Due to the effects of weathering, water impact, and dripping, Pb oxide ore belts form in the upper layers of primary ore deposits. These minerals are very complex, mainly including secondary minerals such as sardinianite (PbSO₄) and cerusite (PbCO₃) [37]. Cerusite is usually derived from sardinianite, which is the direct oxidation product of galena. In most oxidation zones of Pb deposits, a series of other oxygen-containing Pb compounds, including Pb₅(AsO₄)₃Cl [38], vanadinite (Pb₅(VO₄)₃Cl) [39], and crocoite (PbCrO₄), was sometimes generated. Under certain conditions, Pb can combine with limonite or manganese minerals, such as coronadite, and these minerals were also detected.

During smelting, these oxide minerals are heated and reduced by furnace gas, and the majority of Pb oxides are reduced to metallic Pb, which melts at high temperatures and merges with the crude lead. Because Pb is produced under reducing conditions, impurity oxides such as Cu, Sn, and As are also reduced to varying degrees and enriched in the metallic Pb. For example, in the QY002 and QY010 samples, As was detected in the Pb-containing particles by SEM. In addition, in QY010, trace amounts of Cu and Sn were detected, which could combine with Pb to form Cu–Sn–Pb ternary alloy phase particles. By contrast, difficult-to-reduce metal oxides such as FeO, CaO, MgO, Al₂O₃, MnO, and ZnO were mutually fused with SiO₂ at high temperatures to form silicate slag containing zinc oxide and FeO_x–MnO_x–SiO₂ phases, and a Ca-containing slag-forming agent might have been purposefully added during smelting to improve the recovery rate of Pb and, to a certain extent, improve the melting conditions and reduce the melting point.

4. Conclusions

- (1) The slag artefacts comprised silicate phases of Fe, Mn, Ca, and Zn. Most Pb-containing inclusions in the slag were circular, indicating that Pb was added in the molten state. Although the main component of these inclusions was Pb, we note that As, Cu, and Sn were detected in some Pb-containing particles. Therefore, we concluded that these samples comprise the slag discharged after smelting ore for Pb production. In general, the slag can be defined as a FeO_x–MnO_x–SiO₂ slag system. Moreover, a Ca-based slag-forming agent could have been added to reduce the melting point. The main smelting products were crude lead containing a small amount of As, Cu, and Sn.
- (2) The crude lead obtained from smelting might have been directly transported to high-grade sites as the final product or refined to remove As, Cu, and other impurities before being transported.
- (3) Surrounding the Qingyuan site is the Liujiacha–Zuizishan mining area in Pinglu County on the southwestern margin of Zhongtiao Mountains, which includes a polymetallic ore belt and the Bizigou copper mining area, in which Pb, Zn, and Ag deposits are present, and an Mn anomaly has been observed in geochemical profile measurements. Therefore, this area might once have been an ore-mining area and will be the focus of future investigations.
- (4) The plots of the Pb isotope ratios obtained for slag samples from the Qingyuan site and bronze artefacts obtained from the Yanshi Shangcheng site were clustered within the 95% confidence interval. Therefore, we speculate that the lead ores used at the Yanshi Shangcheng site originated from the same location as those at the Qingyuan site. Alternatively, the minerals at the two sites originated from two different sources that were both located in the polymetallic ore belt in the Zhongtiao Mountains.

Author Contributions: Data Curation, methodology, and manuscript review, S.L.; Conceptualization, funding acquisition, and supervision, Y.L.; Funding acquisition and supervision, R.Z.; Formal analysis, writing—review, and editing, H.W. All authors have read and agreed to the published version of the manuscript.

Funding: Program of China (Grant Num. 2020YFC1521606).

Data Availability Statement: Not applicable.

Acknowledgments: We would like to thank Jing Guo (School of Metallurgical and Ecological Engineering, University of Science and Technology and Beijing) for his guidance and comments on this study.

Conflicts of Interest: The authors declare no conflict of interest.

References

- Maddin, R.; Muhly, J.D.; Stech, T. Early metalworking at Çayönü. In *The Beginnings of Metallurgy*; Hauptmann, A., Pernicka, E., Rehren, T., Yalçın, Ü., Eds.; Deutsches Bergbau-Museum: Bochum, Germany, 1999; pp. 37–44.
- Roberts, B. Creating traditions and shaping technologies: Understanding the earliest metal objects and metal production in Western Europe. *World Archaeol.* **2008**, *40*, 354–372. [[CrossRef](#)]
- Odler, M.; Kmošek, J.; Fikrlé, M.; Kochergina, Y.V.E. Arsenical copper tools of Old Kingdom Giza craftsmen: First data. *J. Archaeol. Sci. Rep.* **2021**, *36*, 102868. [[CrossRef](#)]
- Vernet, J.; Ghiara, G.; Piccardo, P. Are tin oxides inclusions in early archaeological bronzes a marker of metal recycling? *J. Archaeol. Sci. Rep.* **2019**, *24*, 655–662. [[CrossRef](#)]
- Meicun, L.; Liu, X. The origins of metallurgy in China. *Antiquity* **2017**, *91*, e6. [[CrossRef](#)]
- Chen, K.; Rehren, T.; Mei, J.; Zhao, C. Special alloys from remote frontiers of the Shang Kingdom: Scientific study of the Hanzhong bronzes from southwest Shaanxi, China. *J. Archaeol. Sci.* **2009**, *36*, 2108–2118. [[CrossRef](#)]
- Mei, J.; Wang, P.; Chen, K.; Wang, L.; Wang, Y.; Liu, Y. Archaeometallurgical studies in China: Some recent developments and challenging issues. *J. Archaeol. Sci.* **2015**, *56*, 221–232. [[CrossRef](#)]
- Ottaway, B.S. Innovation, production and specialization in early prehistoric copper metallurgy. *Eur. J. Archaeol.* **2001**, *4*, 87–112. [[CrossRef](#)]
- Li, J.X. Investigation and Study on Early Copper Mining and Smelting Sites in the South of Shanxi Province, Central. China. Dissertation, University of Science and Technology Beijing, Beijing, China, 2011. (In Chinese).
- Li, Y.X. Initial exploration of early bronze industry layout in the Central Plain and Northern areas in China. *China's Cultural Relics Newspaper*, (In Chinese). 28 February 2014.
- Malik, M.A.; Hassan, M.A.; Qazi, M.A. A method of improving the soundness of lead-free bronze casting. *Adv. Mater.* **1995**, *9*, 159–166.
- Liu, L.; Chen, X. Cities and towns: The control of natural resources in early states, China. *Bull.-Mus. Far East. Antiq.* **2001**, *73*, 5–47.
- Shuyun, S.; Rubin, H.; Murray, J.K. A preliminary study of early Chinese copper and bronze artifacts. *Early China* **1985**, *9*, 261–289. [[CrossRef](#)]
- Liang, H.-G.; Sun, S.-Y.; Li, Y.-X.; Tong, W.-H. A preliminary study of metal particles and mineral phases of copper slag excavated from the Yuanqu City site of the Shang Dynasty. *Sci. Conserv. Archaeol.* **2009**, *4*, 18–30. (In Chinese)
- Liu, Y.; Tang, H.; Liu, J. Pursuing the mineral sources of Yinxu bronze objects (BC13th-BC11th): Study on the lead ingots from Anyang, China. In Proceedings of the 81st Annual Meeting of the Society for American Archaeology, tDAR id: 431610, Vancouver, BC, Canada, 29 March–2 April 2017.
- Li, Y.; Pang, S.; Cheng, J.; Qu, Y.; Cui, C.; Ma, P.; Xia, P.; Hu, X. Investigation of lead smelting sites in Yangxin County, Hubei. *Jiangnan Archaeol.* **2021**, *2*, 101–108.
- Yu, Y.; Chen, J.; Mei, K.; Tie, F. A Preliminary Research of Slag Excavated at Shuzhuangtai, Zhengnan Ancient City Site. *J. Natl. Mus. China* **2012**, *11*, 126–131. (In Chinese)
- Li, Y.X.; Du, N.; Li, J.X. Investigation of Shifotang copper smelting relic site in the Linzi City-site of the Qi State, Shandong Province. *Huaxia Archaeol.* **2014**, *1*, 3–10. (In Chinese)
- Research Center of Field Archaeology. *Survey and Research of Settlement Archaeology in the Eastern Yuncheng Basin*; Science Press: Beijing, China, 2007; p. 114.
- Liu, R. Capturing Changes: Applying the Oxford System to Further Understand the Movement of Metal in Shang China. Ph.D. Thesis, University of Oxford, Oxford, UK, 2016.
- Wu, J.; Zhang, M.L.; Wu, J.M.; Li, Q.J.; Li, J.Z.; Deng, Z.Q.; Jiang, X. Study on the diversification of origins and primary development of Chinese porcelain glazes. *Sci. China Technol. Sci.* **2011**, *54*, 99–104. [[CrossRef](#)]
- Albarède, F.; Desauty, A.-M.; Blichert-Toft, J. A geological perspective on the use of Pb isotopes in archaeometry. *Archaeometry* **2012**, *54*, 853–867. [[CrossRef](#)]
- Komárek, M.; Ettler, V.; Chrástný, V.; Mihaljevič, M. Lead isotopes in environmental sciences: A review. *Environ. Int.* **2008**, *34*, 562–577. [[CrossRef](#)]

24. Melheim, L.; Grandin, L.; Persson, P.-O.; Billström, K.; Stos-Gale, Z.; Ling, J.; Williams, A.; Angelini, I.; Canovaro, C.; Hjärthner-Holdar, E.; et al. Moving metals III: Possible origins for copper in Bronze Age Denmark based on lead isotopes and geochemistry. *J. Archaeol. Sci.* **2018**, *96*, 85–105. [[CrossRef](#)]
25. Yahalom-Mack, N.; Finn, D.M.; Erel, Y.; Tirosch, O.; Galili, E.; Yasur-Landau, A. Incised Late Bronze Age lead ingots from the southern anchorage of Caesarea. *J. Archaeol. Sci. Rep.* **2022**, *41*, 103321. [[CrossRef](#)]
26. Dong, J.-M.; Zhao, F.; Zhang, Y.-L.; Qiu, S.-T.; Gan, Y. Distribution behaviors of vanadium between hot metal and FeO-SiO₂-MnO-(TiO₂) slag system and influential factors. *Chin. J. Process Eng.* **2010**, *10*, 1076–1083. (In Chinese)
27. Jin, Z. *Lead Isotopes Archaeology in China*; Press of University of Science and Technology of China: Hefei, China, 2008; p. 26.
28. Dazhong, S.; Weixing, H.; Min, T.; Fengqing, Z.; Condie, K.C. Origin of Late Archean and Early Proterozoic rocks and associated mineral deposits from the Zhongtiao Mountains, east-central China. *Precambrian Res.* **1990**, *47*, 287–306. [[CrossRef](#)]
29. Qiu, Z.-J.; Fan, H.-R.; Liu, X.; Yang, K.-F.; Hu, F.-F.; Xu, W.-G.; Wen, B.-J. Mineralogy, chalcopyrite Re–Os geochronology and sulfur isotope of the Hujiayu Cu deposit in the Zhongtiao Mountains, North China Craton: Implications for a Paleoproterozoic metamorphogenic copper mineralization. *Ore Geol. Rev.* **2016**, *78*, 252–267. [[CrossRef](#)]
30. He, Y.; Zhao, G.; Sun, M.; Wilde, S.A. Geochemistry, isotope systematics and petrogenesis of the volcanic rocks in the Zhongtiao Mountain: An alternative interpretation for the evolution of the southern margin of the North China Craton. *Lithos* **2008**, *102*, 158–178. [[CrossRef](#)]
31. Fan, C.; Yu, Z. *Zhongtiaoshan Precambrian Hujiayu-Bizigou Type Copper Mine*; Tianjin Science Research Association: Tianjin, China, 1997; p. 21. (In Chinese)
32. Yun, K. *Special Report on Geological Methods of Copper-Lead-Zinc Polymetallic Mine in Guanxigou Area, Pinglu County, Shanxi Province (File No.: Cgdoi.n0001/x001043300)*; Shanxi Physical and Chemical Institute of Geology and Mineral Exploration Company; North China Geological Bureau: Yuncheng, China, 2004. (In Chinese)
33. Li, H.J.; Liu, S. Study on metallogenic geological background of copper polymetallic deposit in central and southern Zhong-tiao Mountains, Shanxi. *Sci. Wealth* **2015**, *7*, 1. (In Chinese)
34. Li, H.J. Metallogenic Regularity and Prospecting Direction of Copper Polymetallic Deposits in Middle South of Zhongtiao Mountain, Shanxi Province. Master's Thesis, Hebei GEO University, Shijiazhuang, China, 2016. (In Chinese).
35. Mernagh, T.P.; Trudu, A.G. A laser Raman microprobe study of some geologically important sulphide minerals. *Chem. Geol.* **1993**, *103*, 113–127. [[CrossRef](#)]
36. Geological Department in North China. *Overview of Lead, Zinc and Silver (File No.: Cgdoi.n0001/x00010931)*; The National Geological Archives: Beijing, China, 1956. (In Chinese)
37. Buckley, A.N.; Woods, R. An X-ray photoelectron spectroscopic study of the oxidation of galena. *Appl. Surf. Sci.* **1984**, *17*, 401–414. [[CrossRef](#)]
38. Lalinská-Voleková, B.; Majzlan, J.; Klimko, T.; Chovan, M.; Kučerová, G.; Michňová, J.; Hovorič, R.; Göttlicher, J.; Steininger, R. Mineralogy of weathering products of Fe–As–Sb mine wastes and soils at several Sb deposits in Slovakia. *Can. Mineral.* **2012**, *50*, 481–500. [[CrossRef](#)]
39. Frost, R.L.; Crane, M.; Williams, P.A.; Klopogge, J.T. Isomorphic substitution in vanadinite [Pb₅(VO₄)₃Cl]—A Raman spectroscopic study. *J. Raman Spectrosc.* **2003**, *34*, 214–220. [[CrossRef](#)]

Disclaimer/Publisher's Note: The statements, opinions and data contained in all publications are solely those of the individual author(s) and contributor(s) and not of MDPI and/or the editor(s). MDPI and/or the editor(s) disclaim responsibility for any injury to people or property resulting from any ideas, methods, instructions or products referred to in the content.